

Dynamic Response Analysis of Ash Dyke and Evaluation of Different Construction Methods

Durgesh Kumar¹, Siddhardha R¹ [0000-0001-8696-6583], Debdip Das¹, Kalyan Kumar Gonavaram¹ [0000-0002-5803-7338]

¹Department of Civil Engineering, NIT Warangal, Telangana, India
dkce20223@student.nitw.ac.in, rs721001@student.nitw.ac.in,
ddce21213@student.nitw.ac.in, kalyan@nitw.ac.in

Abstract. The large disposal problem of fly ash can be minimized by using it to the maximum possible extent in the various geotechnical fields. When it is used in the geotechnical applications such as construction of ash dykes in the earthquake prone regions, maintaining its stability becomes a major concern because earthquake induced instability can cause large lateral spreading of the ash material. Due to the inertia of height raised ash dykes, earthquake generates significant horizontal and vertical forces. This allows the amount of particulate material to decrease its volume, causing a rise in pore pressure, a decrease in the strength of the soil, leading to partial or complete collapse of the ash dykes. Mitigation of this problem requires a profound understanding of its dynamic behavior. In addition to this, different methods of raising ash dyke largely affects the performance of dyke during a seismic event. A dynamic response study and an analysis of the developing instability, which can be described in terms of amplification or displacement, are necessary for evaluating the performance of ash dykes under seismic loading circumstances. In this study, suitability of the methods of raising ash dyke is proposed under the dynamic conditions. Efforts are made to perform dynamic response analysis of ash dyke by determining the amount of displacement and amplification in the ash dyke when it is subjected to earthquake motions. From dynamic response analysis of the ash dyke, it is obtained that the earthquake induced displacement of the dykes can be as high as 4-5 m and in the staged construction of ash dyke, upstream method of construction may not be a good alternative to be used in the earthquake prone regions.

Keywords: Fly ash, Experimental data, Plaxis2D, Earthquake data.

1 Introduction

India is the fifth largest coal reserve in the world, and more than 70% of the country's electricity is produced from coal (Singh et al. 2019). In the coal-based Thermal Power Plants, 80% of fly ash and 20% of bottom ash is produced. Fly ash is widely available, demonstrating its exceptional usage in structural fills and several geotechnical applications. In India, highest level of utilization of about 83.05% is achieved during 2019-2020 in the various fields such as cement, ash dyke raising, brick and tile manufacturing, reclamation of low-lying area etc. Conventionally the unutilized volume of fly ash is mixed with large amount of water, and deposited in the Pond Ash. Pond ash deposits

have already covered 65000 acres of land in India (Parswal et al. 2003) and many million acres all over the world. This disposal problem needs to be minimized by using it to the maximum possible extent. However, the utilization of fly ash requires profound understanding of its static and dynamic behavior, especially if it is used in the construction of ash dykes in seismic prone regions, where transporting other materials from another source is uneconomical. In the static condition it behaves similar to the natural cohesionless soil, but due to their less unit weight and high porosity, the behavior of the ash materials under dynamic loading could be different from natural soils depicting the importance of detailed examination of its dynamic characteristics. Due to the inertia of heigh raised ash dykes, earthquake generates significant horizontal and vertical forces, as well as highly irregular ground motion. Response of ash dyke during an earthquake event is highly dependent on particle behavior of the fly ash.

2 Materials and Methods

The performance of ash dykes during earthquake loading conditions can be affected by the static and dynamic properties of fly ash. The finely divided byproduct of burning pulverized coal is known as fly ash. Hence, material characterization is an important step in the dynamic study of ash dyke. In this study, material properties of fly ash are determined from the experimental investigation as furnished in Table 2.1 and from the numerical analysis, dynamic response of the ash dyke is determined in terms of amplification and displacement. In the analysis part natural frequency of the ash dyke is determined and then a set of earthquake data is selected to cover a good range of frequency for the dynamic response analysis. To determine the effect of vertical motion a single stage dyke is considered and analysed using horizontal and vertical components of the earthquakes. From the dynamic response analysis of the ash dyke following U/S and D/S method of construction, the suitability of the method for the construction of ash dykes in the earthquake prone region is determined. Fly ash is a by-product obtained from bituminous or sub-bituminous coal based thermal power plants. The behaviour observed in the laboratory test helps to understand material performance in the field and can predict the behaviour of field structures constructed with the fly ash. In the present study fly ash collected from the National Aluminium Company Limited (NALCO), Angul Thermal Power Plant, Odisha, is used.

Table 2.1. Grain size analysis result.

Properties	Values
Sand size (4.75 – 0.075 mm) (%)	24
Silt size (0.075 – 0.002 mm) (%)	68
Clay size (< 0.002 mm) (%)	8
D60 size (mm)	0.062
D30 size (mm)	0.017
D10 size (mm)	0.005
Uniformity coefficient, Cu	12.33
Coefficient of curvature, Cc	0.78

2.1 Numerical study

The use of numerical models to analyse nonlinear material behaviour and its interaction with geotechnical structures has become prevalent. In the present study, analysis is performed using a plane strain finite element method in the PLAXIS2D. This numerical tool provides different material models that describes how the force displacement relationship is enforced into the analysis. Among different material models, Mohr Coulomb material model is used for the study. The methodology adopted for finding the natural frequency of the ash dyke using time history analysis. The principle of finding natural frequency is based on the idea that the embankments have tendency to filter those seismic waves, whose predominant frequency is far away from the natural frequency of the dam. Hence, in order to consider a wide range of frequency, a synthetic sine wave generated in MATLAB (MathWorks Inc., 2015), containing sinusoidal wave of different frequencies ranging from 0.01 – 10 Hz with an increment of 0.02 for a time duration of 13.28 sec is considered in the analysis. Geometry of the ash dyke considered in the analysis is pond ash embankment at Renusagar thermal power plant, Uttar Pradesh, India. The region of the considered ash dyke comes in the seismic zone-III as per IS 1893 – Part 1 (2016), where moderate level of seismicity can be expected which shows the significance of conducting dynamic response analysis of the Renusagar pond ash embankment. Embankment has a total height of 52 m which is the highest pond ash embankment in India. Side slopes are 2.5H: 1V and the depth of ground water table is at 7.5 m from the crest of the embankment. Foundation soil consists of 27 m depth of silty sand overlain by bedrock. CPT test data has shown the medium dense ash deposit as well as medium dense foundation soil (Vijaysaree et al. 2017). In the FE analysis, geometry was drawn comprising of first 27 m of foundation soil and then dam having 52 m in height resting on foundation soil is created as shown in Fig. 2.1.

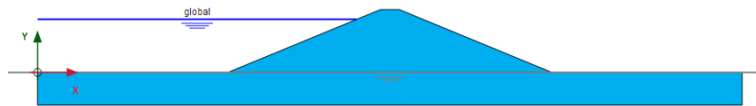


Fig. 2.1. Finite element model of the ash dyke

2.2 Collection of earthquake data

Earthquake data used in the analysis is selected from the two sources. Six sets of data are collected from Consortium of Organizations for Strong Motion Observation Systems (COSMOS) database. The second source is the ground motion database of the Pacific Earthquake Engineering Research Centre (PEER) that contains a large number of ground motions recorded at shallow depth all over the world. To consider different levels of seismic excitations, a total of 17 earthquake data is used in this study. Both horizontal and vertical component of the recorded earthquakes with the PGA, PGV, PGD, Predominant frequency (f_p) are shown in Table 2.2, and the same motions with Arias Intensity, Sustained Maximum Acceleration (SMA) values determined using Seismosignal software are presented in the Table 2.2. Considered motions consists of a

range of PGA from 0.062-1.177 (g), PGV from 0.019-1.209 m/s and PGD from 0.005-0.718 m. Depending on the natural frequency of the considered ash dyke, total earthquake data has been divided into three groups A, B, and C, to study the effect of frequency content of an earthquake motion on the dynamic response. Group A, B and C contains the earthquake data having low, intermediate and high predominant frequencies respectively. Predominant frequencies of group B are close to the natural frequency of the ash dyke.

Table 2.2. Ground motion parameters

Motion Name	Horizontal Component				Vertical Component			
	PGA (g)	PGV (m/s)	PGD (m)	fp (Hz)	PGA (g)	PGV (m/s)	PGD (m)	fp (Hz)
Chamoli	0.062	0.096	0.718	2.64	0.22	0.321	1.20	2.39
Xizang	0.076	0.0186	0.0683	4.10	0.031	0.011	0.0415	4.2
Bhuj	0.104	0.1105	0.183	1.17	0.069	0.042	0.189	3.96
Blue lake	0.105	0.063	0.006	1.92	0.034	0.016	0.000	2.16
Chamba	0.143	0.073	0.0575	2.93	0.083	0.046	0.072	1.95
India Burma	0.159	0.224	0.135	1.78	0.033	0.020	0.0227	4.00
Kalamata	0.161	0.128	0.013	3.46	0.08	0.047	0.009	1.074
Hecter mine	0.186	0.232	0.052	1.94	0.119	0.088	0.042	1.93
Bombay Beach	0.234	0.069	0.005	4.14	0.089	0.012	0.003	16.49
Uttarkashi	0.248	0.166	0.592	1.97	0.289	0.177	1.602	4.27
Palm Spring	0.294	0.328	0.068	1.66	0.54	0.191	0.347	5.59

3 Result and Discussion

3.1 Displacement results

Fig. 3.1 and Fig. 3.2 shows the displacement contours of the ash dyke models constructed using upstream and downstream method of constructions respectively. For the applied horizontal motion of Kalamata earthquake having PGA of 0.16(g), deformation is measured. It can be seen that the total displacement of the ash dyke constructed using upstream and downstream methods are 2.176 m and 0.203 m respectively. In case of upstream method, displacement of 2.176 m exceeds the value of 1 m suggested by Gujarat State Disaster Management Authority (GSDMA), whereas the displacement value of 0.203 m in downstream method is well below 1 m.

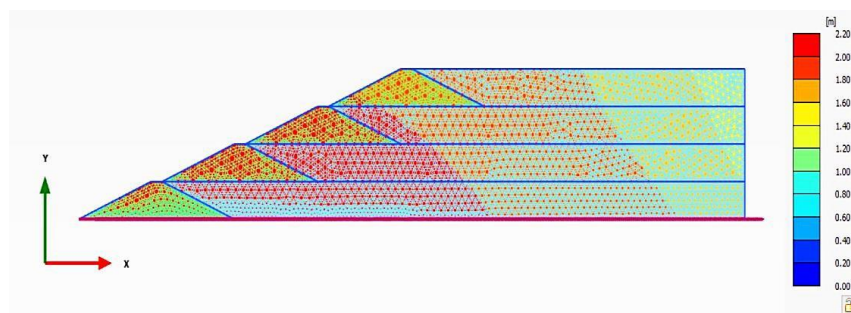


Fig. 3.1. Deformed shape of ash dyke constructed using U/S method

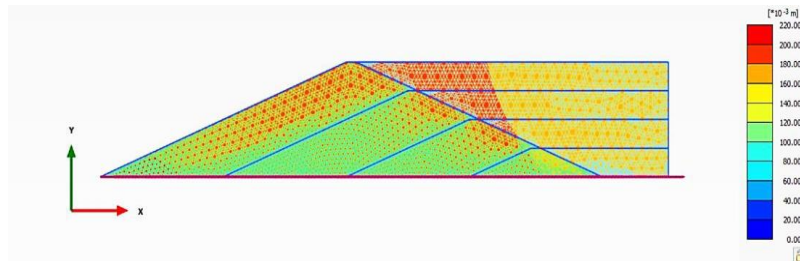


Fig. 3.2. Deformed shape of ash dyke constructed using D/S method

3.2 Acceleration response results

Fig. 3.3 shows the variation of peak spectral acceleration demand of the ash dykes for upstream method of construction. For the applied horizontal motion of Kalamata earthquake having PGA of 0.16(g), response is measured at 5% of damping for the period of 10 seconds at the final construction stage of the ash dyke.

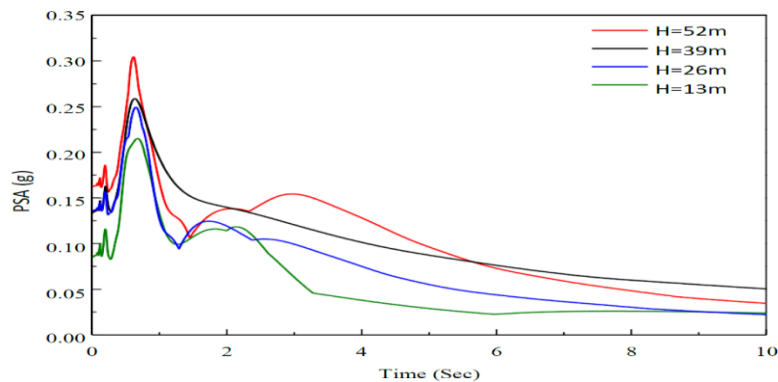


Fig. 3.3 Peak spectral acceleration demand of the ash dyke constructed using upstream method of construction.

3.3 Effect of PGA

The most fundamental and commonly used intensity index for seismic structural analysis is the PGA, which is also used in many structural design codes or standards all over the world. The effect of PGA of the input motions are discussed in the section below.

Horizontal Component

Fig. 3.4 shows the variation of maximum horizontal and vertical displacement of ash dyke with the PGA of different input motions ranging from 0.062 (g) to 1.177 (g). The maximum horizontal displacement is found to be 496 mm for input motion Chamoli

having lowest PGA_x of 0.062 (g) and the minimum horizontal displacement is found to be 39 mm for motion Loma Prieta having highest PGA_x of 1.177 (g). The vertical displacement (U_y) of the dyke is found to be lesser than that of the horizontal displacement (U_x) at all PGA_x values, and it is maximum for Northridge earthquake having a PGA_x of 0.852 (g). It should be noted that the displacement values do not follow any pattern with the PGA_x of the input motions and deviate randomly as the PGA_x increases.

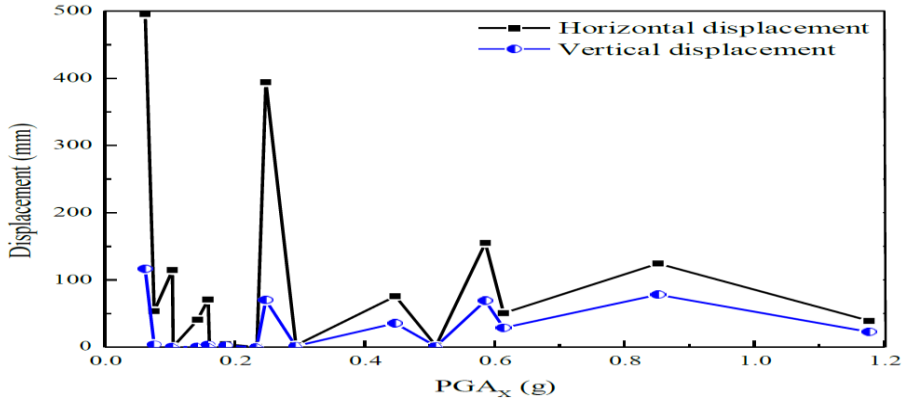


Fig. 3.4. Variation of maximum displacement of dyke with PGA of horizontal component of earthquake.

Combined horizontal and vertical components

Fig. 3.5 shows the variation of the maximum horizontal and vertical displacement of the ash dyke with the combined PGA of horizontal and vertical components of different input motions. In the plot, PGA_{xy} denotes the combined PGA of horizontal and vertical component of the input motions, which is taken as geometric mean of both the components.

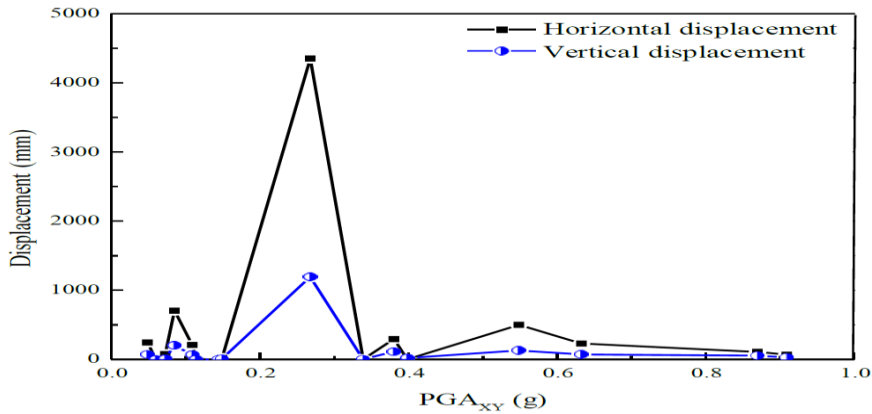


Fig. 3.5. Variation of maximum displacement of dyke with combined PGA of horizontal and vertical component of earthquake

The plot shows that the both horizontal and vertical displacement components are increased due to inclusion of vertical component. Fig. 3.5 shows the maximum horizontal and vertical displacement of 4351 mm and 1194 mm, which exceeds the allowable value of 1m as suggested by GSDMA. The highest U_x and U_y values are observed for the same motion Uttarkashi, which has a PGA_{XY} of 0.267 (g).

3.4 Effect of predominant frequency

Displacement results obtained from the finite element method, using sinusoidal wave of different predominant frequencies are presented in this section. The maximum horizontal displacement of the embankment is compared with some classical deformation analysis results. Fig. 3.6 shows the result of deformation analysis superimposed with the results of other numerical and analytical methods found in the literature (Jafarzadeh et al., 2015). Present study shows that the maximum horizontal displacement value ranges from 138 cm to 18 cm for the change in frequency between 1 Hz to 10 Hz.

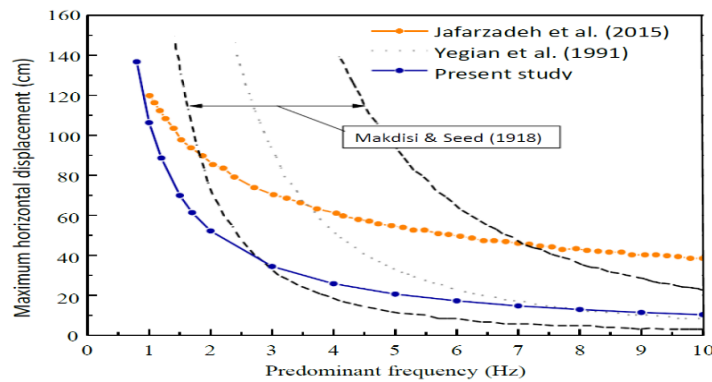


Fig. 3.6. Variation of displacement with predominant frequency (Hz)

Jafarzadeh's numerical model results fit the present result extremely well at lower predominant frequencies. However, at the maximum considered predominant frequency of 10 Hz, the F. Jafarzadeh's numerical model produces a displacement value of 40 cm, which is an overestimation of displacement as compared to all other approaches. It can also be seen that, at frequencies greater than 2.5 Hz, the displacement values of the current study are within the range of analytical findings (Yegian et al. 1991; Makdisi and seed, 1918). Displacement Analysis results using sinusoidal motion gives an important observation regarding the dependency of displacement on the predominant frequency. However, it is unable to represent the actual displacement response of the dyke when it is subjected to real earthquake motion.

Horizontal component

Fig. 3.7 shows the variation of earthquake induced displacement with the ratio of predominant frequency of input motion to natural frequency of vibration in horizontal direction. It can be seen that the displacement is higher for the input motions Chamoli and Uttarkashi having predominant frequencies of 2.64 Hz and 1.97 Hz, thereby giving

frequency ratio of 1.32 and 0.99 respectively. It is well understood that, when the predominant frequency of the input motion coincides with the natural frequency of the structure, response in a structure gets amplified. Hence, higher value of displacement in case of Chamoli and Uttarkashi motions is in line with the above theory.

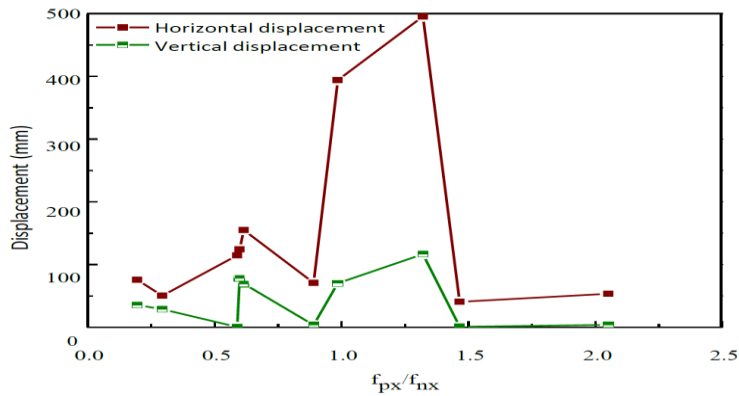


Fig. 3.7. Variation of displacement with predominant frequency of the motion normalized with the natural frequency in horizontal direction

Combined horizontal and vertical component

Fig. 3.8 shows the variation of displacement with the ratio of predominant frequency of the vertical motion to that of horizontal motion (f_{py}/f_{px}), i. e. frequency ratio.

It is observed that the displacement values are prominent at the lower frequency ratio and as frequency ratio increases, it becomes lesser. Hence, earthquake motion having lower frequency ratio (comparable horizontal and vertical predominant frequency) can cause more deformations however, damage caused by an earthquake having higher frequency ratio may not be very significant. From the frequency-based analysis, it can be observed that the same ash dyke when subjected to sinusoidal motion of varying frequency gives a maximum displacement of around 150 cm whereas, when it is subjected to real earthquake motion, the displacement values can be excessively high.

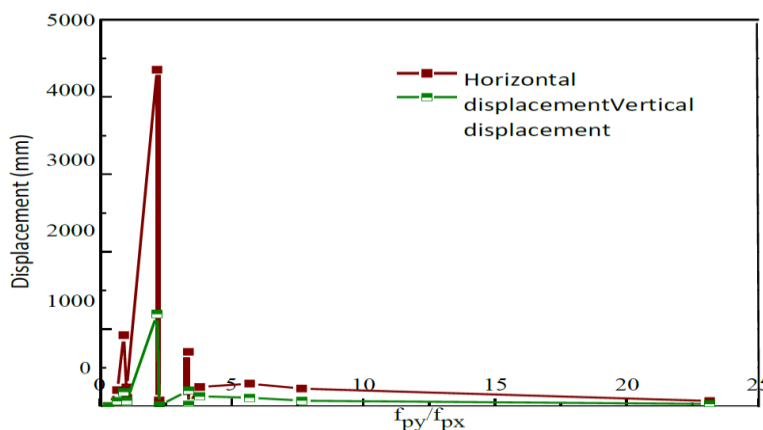


Fig. 3.8 Variation of displacement with frequency ratio of the motion

3.5 Effect of PGD

To examine the influence of PGD of applied earthquake motion in the response of the ash dyke in terms of displacement, the same measured displacement of different input motions used in the previous PGA study are plotted with the PGD. Fig. 3.10 shows the variation of maximum horizontal and vertical displacement of ash dyke with the PGD of different input motions ranging from 6 mm to 718 mm. In this plot PGD_x denotes the PGA of only horizontal component of the earthquakes. It can be noted that the maximum horizontal and vertical displacement value increases with increase in PGD_x for all input motions. Unlike the case of PGA, the displacement of the ash dyke shows a strong correlation with the PGD_x of the input motions. Fig. 3.11 shows the variation of the maximum horizontal and vertical displacement of the ash dyke with the combined PGD of horizontal and vertical components of different input motions. Highest value of maximum horizontal and vertical displacement is found for motion Uttarkashi having a PGD_{xy} of 974 mm. According to the results of the analysis of earthquake-induced maximum lateral and vertical displacement of the dyke, there is a clear association between the displacement of the dyke and the PGD value of the input motions.

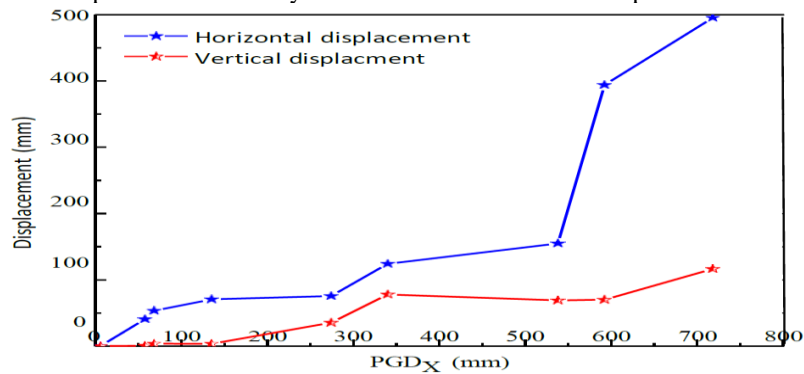


Fig. 3.10. Variation of maximum displacement of dyke with PGD of horizontal component of earthquake

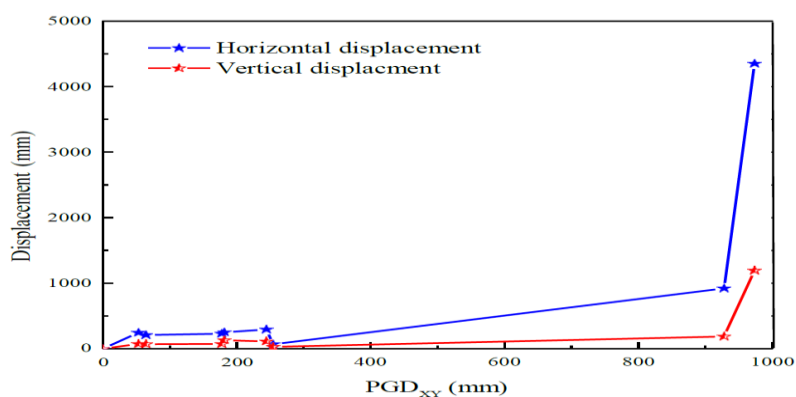


Fig. 3.11. Variation of maximum displacement of dyke with combined PGD of horizontal and vertical component of earthquake

3.6 Acceleration Response

Fig. 3.12 shows the acceleration response in terms of amplification throughout the height of the ash dyke for horizontal component of the considered earthquake motions. H represents total height of the ash dyke and z is the depth considered from the crest of the dyke. Amplification is measured as the ratio of maximum acceleration recorded at any depth z to the maximum acceleration applied at the base of ash dyke. $(A_{max}/A_{base})_X$ represents the amplification by considering only horizontal component of the motion. From Fig. 3.12, it is observed that maximum amplification occurs at the crest point for all input motions. Range of amplification is 0.92 - 3.24 for the considered range of PGA of 0.062g to 1.177g. Motion having predominant frequency (f_p) close to the natural frequency (f_n) of the ash dyke shown highest amplification whereas, the one with predominant frequency far away from natural frequency of the dyke, shown the lower amplification throughout the height of the embankment.

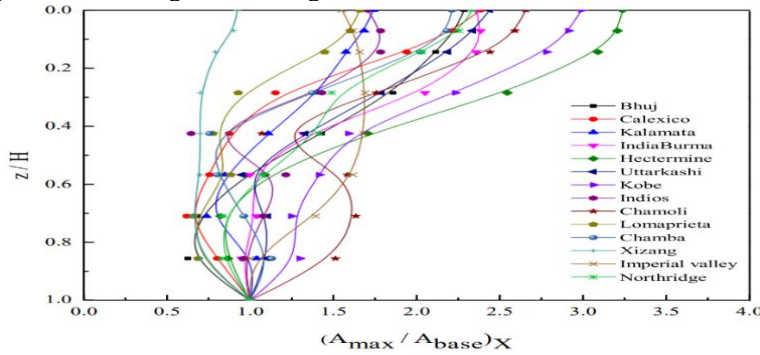


Fig. 3.12. Variation of acceleration amplification throughout the height of ash dyke considering horizontal component of the input motion

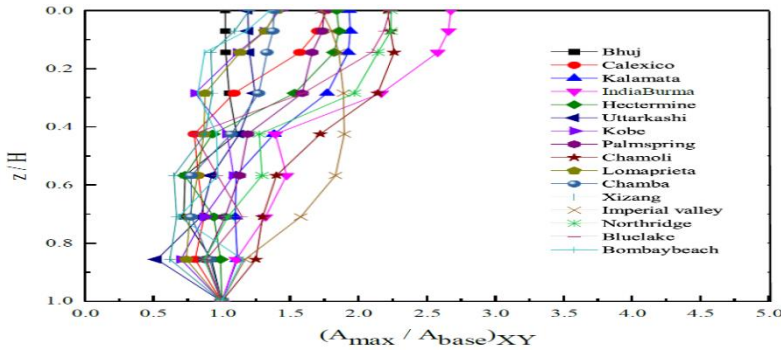


Fig. 3.13. Variation of acceleration amplification throughout the height of ash dyke considering horizontal and vertical component of the input motions

4 Conclusion

It is undoubtedly true that ground motion triggered at an ash dyke site by an earthquake will cause the dyke and their associated facilities to be damaged. It is seen that the earthquake induced displacement of the ash dyke can be as high as 4-5 m. The major

outcomes of the dynamic response analysis of the ash dyke performed using FEM can be concluded in the following points:

- Effect of vertical component of the input motion is significant in the response of the ash dyke and can lead to excessive deformations. Hence it should be considered in the design especially if the dyke is constructed in a region where earthquake of strong horizontal and vertical components is likely to occur.
- After analyzing the response of ash dyke for a large number of earthquake motion with PGA ranging from 0.062(g)-1.177(g), the range of amplification for the combined motion is proposed as 1.026-2.67.
- Higher spectral acceleration demand of the upstream method of construction confirms that despite being economical method, it is not suitable to be used in the seismically active regions.

References

1. A. J., & Verreault, L. (2018). Use of constant energy source in SASW test and its influence on seismic response analysis. *Geotechnical Testing Journal*, 41(6), 1102-1116.
2. Ali, A., De Risi, R., Sextos, A., Goda, K., & Chang, Z. (2020). Seismic vulnerability of offshore wind turbines to pulse and non-pulse records. *Earthquake Engineering & Structural Dynamics*, 49(1), 24-50.
3. Ambraseys, N. N., & Menu, J. M. (1988). Earthquake-induced ground displacements. *Earthquake engineering & structural dynamics*, 16(7), 985-1006.
4. Ancheta, T. D., Darragh, R. B., Stewart, J. P., Seyhan, E., Silva, W. J., Chiou, B. S., ... & Donahue, J. L. (2013). Peer NGA-West2 database.
5. Anderson, D. G. (2008). Seismic analysis and design of retaining walls, buried structures, slopes, and embankments. Transportation Research Board, 611.
6. ASTM, D. (2011). Standard Test Method for Consolidated Drained Triaxial Compression Test for Soils (D7181-11). ASTM International, West Conshohocken, Pa.
7. Banerjee, A. (2017). Response of unsaturated soils under monotonic and dynamic loading over moderate suction states (Doctoral dissertation).
8. Barberopoulou, A., Qamar, A., Pratt, T. L., Creager, K. C., & Steele, W. P. (2004). Local amplification of seismic waves from the Denali Earthquake and damaging seiches in Lake Union, Seattle, Washington. *Geophysical research letters*, 31(3).
9. Bray, J. D. (1990). The effects of tectonic movements on stresses and deformations in earth embankments (Doctoral dissertation, University of California, Berkeley).
10. Central Electricity Authority (2014). Report on fly ash generation at coal / lignite based thermal power stations and its utilization in the country for the year 2019 – 20.
11. Chakraborty, S., Das, J. T., Puppala, A. J., & Banerjee, A. (2019). Natural frequency of earthen dams at different induced strain levels. *Engineering Geology*, 248, 330-345.
12. Faiz I. Makdisi , and H. Bolton Seed (1978), Simplified procedure for estimating dam and embankment earthquake-induced deformations *Journal of the Geotechnical Engineering Division*, 104(7): 849-67.
13. Fardin Jafarzadeh, Mohammad Mahdi Shahrabi, Hadi Farahi Jaromi (2015). On the role of topographic amplification in seismic slope instabilities. *Journal of Rock Mechanics and Geotechnical Engineering*, 7(2): 163-170.

14. Hall, J. F., & Chopra, A. K. (1982). Hydrodynamic effects in earthquake response of embankment dams. *Journal of the Geotechnical Engineering Division*, 108(4), 591-597.
15. Parswal, I. S., Makan, O. P., & Atrea, A. K. (2003). Eco friendly ash management in the form of ash mound.
16. Seed, H. B., & Lee, K. L. (1966). Liquefaction of saturated sands during cyclic loading. *Journal of the Soil Mechanics and Foundations Division*, 92(6), 105-134.
17. Singh, S., & Pillai, A. (2019). A Compressive Review on Fly Ash Characteristics and Current Utilization Status in India. In *Proceedings 2019: Conference on Technologies for Future Cities (CTFC)*.
18. Sridharan, A., & Prakash, K. M. (2007). *Geotechnical engineering characterisation of coal ashes*. CBS Publishers & Distributors.
19. Vijayasri, T., Raychowdhury, P., & Patra, N. R. (2017). Seismic response analysis of Renusagar pond ash embankment in Northern India. *International Journal of Geomechanics*, 17(6), 04016141.
20. Yegian, M. K., Marciano, E. A., Ghahraman, V. G. (1991). Earthquake-induced permanent deformations: probabilistic approach. *Journal of Geotechnical Engineering*, 117(1), 35-50.